

Quantum phase estimation by compressed sensing

Changhao Yi^{1,2}, Cunlu Zhou³, and Jun Takahashi³

¹State Key Laboratory of Surface Physics and Department of Physics, Fudan University, Shanghai 200433, China

²Institute for Nanoelectronic Devices and Quantum Computing, Fudan University, Shanghai 200433, China

³Center for Quantum Information and Control, Department of Physics and Astronomy, University of New Mexico, NM 87131, USA

As a signal recovery algorithm, compressed sensing is particularly useful when the data has low-complexity and samples are rare, which matches perfectly with the task of quantum phase estimation (QPE). In this work we present a new Heisenberg-limited QPE algorithm for early quantum computers based on compressed sensing. More specifically, given many copies of a proper initial state and queries to some unitary operators, our algorithm is able to recover the frequency with a total runtime $\mathcal{O}(\epsilon^{-1} \text{poly log}(\epsilon^{-1}))$, where ϵ is the accuracy. Moreover, the maximal runtime satisfies $T_{\max} \epsilon \ll \pi$, which is comparable to the state of art algorithms, and our algorithm is also robust against certain amount of noise from sampling. We also consider the more general quantum eigenvalue estimation problem (QEEP) and show numerically that the off-grid compressed sensing can be a strong candidate for solving the QEEP.

1 Introduction

Quantum phase estimation (QPE) [1] is one of the most useful subroutines in quantum computing and plays an important role in many promising quantum applications [2, 3, 4, 5]. Given a unitary matrix U and one of its eigenvectors $|\Phi\rangle$ such that $U|\Phi\rangle = e^{2\pi i\theta}|\Phi\rangle$, the task of QPE is to estimate θ with high probability within a given accuracy guarantee. The problem of estimating multiple phases (or eigenvalues) of U has been referred to the quantum eigenvalue estimation problem (QEEP) [6, 7, 5, 8, 9]. While fully fault-tolerant quantum computers may still be years away from realizing, early fault-tolerant quantum computers with limited number of logical qubits and circuit depth, are expected to be realized much sooner and are expected to solve nontrivial tasks that demonstrate true practical quantum advantages. Given the crucial role of QPE in many of such tasks, it becomes imperative to design QPE algorithms specifically tailored for early fault-tolerant quantum computers.

The standard textbook QPE algorithm [10] does not require an exact eigenstate as the initial state and takes only one measurement, but it uses $\mathcal{O}(\log(\epsilon^{-1}))$ ancilla qubits and controlled operations, which is fairly demanding for early fault-tolerant quantum computers. While Kitaev's original iterative QPE algorithm [1] only uses one ancilla qubit and one controlled operation (see Fig. 1), it requires the initial state to be an exact eigenstate which can be a difficult task by itself. Much of the recent work [7, 11, 12] in QPE for early fault-tolerant quantum computers has focused on designing better classical post-processing

algorithms to improve various aspects of Kitaev’s original QPE algorithm. More specifically, the following properties are desired in designing such algorithms:

- The quantum circuit should be simple, using at most one ancilla qubit and one controlled operation.
- The initial state is not necessarily an exact eigenstate.
- The total runtime achieves the Heisenberg limit, i.e., the total cost should be $\mathcal{O}(\epsilon^{-1} \text{poly log}(\epsilon^{-1} \delta^{-1}))$ for estimating the phase to accuracy ϵ with probability $1 - \delta$.
- When the overlap of the initial state and the targeted eigenstate is large, the maximal runtime T_{\max} (hence the maximum circuit depth) can be much smaller than π/ϵ .

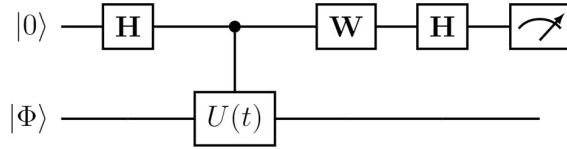


Figure 1: The one-ancilla quantum circuit used in Kitaev-type QPE algorithms. **H** is the Hadamard gate, and the measurement is in Z basis. In terms of the measurement outcome, we regard the $|0\rangle$ state as obtaining value $+1$, and the $|1\rangle$ state as obtaining value -1 . When $\mathbf{W} = I$, the measurement outcome is ± 1 with probability $(1 \pm \text{Re}(\langle \Phi | U(t) | \Phi \rangle))/2$ respectively. When $\mathbf{W} = S^\dagger$, the complex conjugation of the phase gate, the measurement outcome is ± 1 with probability $(1 \pm \text{Im}(\langle \Phi | U(t) | \Phi \rangle))/2$ instead. After taking the average over many test outcomes, we obtain an estimate of the true signal $\langle \Phi | U(t) | \Phi \rangle$.

Kitaev’s original iterative QPE algorithm is a hybrid quantum algorithm. The quantum part is a combination of Hamiltonian simulation and the Hadamard test (see Fig. 1). Hamiltonian simulation algorithms [13] are used to prepare the unitary operator $U(t)$ where longer evolution time requires more quantum gates. The best known circuit complexity for running $U(t)$ without ancilla qubits is almost linear using higher order Trotter-Suzuki formula methods [14, 15]. The Hadamard test then produces information about $U(t)$ in the form of a complex signal. Specifically, given an initial state $|\Phi\rangle$, $\langle \Phi | U(t) | \Phi \rangle$ can be estimated with many runs of Hadamard tests. In QPE, the signal $\langle \Phi | U(t) | \Phi \rangle$ is dominated by a single sinusoidal function, and we aim to estimate its frequency. In QEEP, the signal is regarded as a linear combination of multiple principle sinusoidal functions.

The classical part of the QPE and QEEP is then to estimate the frequencies from these statistically sampled signals, which is very similar to what signal recovery algorithms aim for. In [7], a Fourier filter function was used to estimate the ground-state energy with Heisenberg-limit scaling which works for any initial state with $p_0 > 0$, where p_0 is the overlap between the initial state and the eigenstate. When the overlap p_0 is large, the work of [11] further reduced the prefactor $\beta = T_{\max} \epsilon$ in the maximum running time (i.e., the maximum circuit depth) β/ϵ by using a subroutine called the quantum complex exponential least squares (QCELS). In contrast to [7] in which the prefactor is independent of the initial overlap p_0 and is at least π , the prefactor in [11] can be arbitrarily close to 0 ($\beta = \sqrt{\Theta(1 - p_0)}$) as $p_0 \rightarrow 1$ when $p_0 > 0.71$. It is also worth mentioning that the more recent work [12], which is based on the robust phase estimation result in [16, 17], further improved this overlap to $p_0 > 0.536$ and the prefactor in the maximum running time to $\delta = \Theta(1 - p_0)$ as $p_0 \rightarrow 1$. In [18] and [19], the last two QPE algorithms have been extended to the QEEP, i.e., the multiple-phase estimations.

In this work we present a new paradigm of solving both QPE and QEEP with compressed sensing [20, 21, 22], which has not been carefully considered as far as we know. Compressed sensing is a prominent algorithm for signal recovery, which has been widely applied to various domains such as time-frequency analysis, image processing, and quantum state tomography [23, 24]. The framework of compressed sensing assumes the sparsity of the signal and recovers the entire signal from a few samples by solving a linear/semidefinite programming (SDP) problem. Here, the sparsity refers to the number of nonzero frequencies being small (typically $\mathcal{O}(1)$). The small number of required samples and its robustness makes compressed sensing a strong candidate for solving the phase estimation problem.

Our main contribution is a simple and robust classical post-processing algorithm for QPE based on compressed sensing. In QPE we may regard both the uncertainty from the Hadamard tests and the inaccuracy of initial state preparation as noise. To extract target frequency f_0 in presence of noise, our main idea is using the robust recovery property of convex relaxation algorithm [21], a modified version of the vanilla compressed sensing. For signal vectors with size N , when the frequency f_0 is nearly on-grid ($f_0 \approx n/N$) and the noise for each sample is bounded by a constant, the convex relaxation algorithm can recover f_0 in accuracy N^{-1} with only $\mathcal{O}(\log N)$ samples, which satisfies the Heisenberg limit. With no prior knowledge about f_0 (i.e., f_0 could be off-grid), our algorithm can still find a grid shift parameter ν such that after shifting the signal by $e^{i2\pi\nu t/N}$, the new signal becomes nearly on-grid, and the convex relaxation algorithm still works. The accuracy of f_0 can thus be improved from N^{-1} to αN^{-1} , where α is a constant related to the noise. In terms of the maximum runtime T_{\max} , or equivalently the maximum circuit depth, since the samples of the compressed sensing algorithm are integers from $[1, N]$, T_{\max} scales linearly in N . For the more general QEEP problem, the regular compressed sensing algorithm is not ideal because it is not guaranteed that all frequencies are nearly on-grid simultaneously. Instead we will consider the off-grid compressed sensing framework [25, 26], which outputs the estimate of time domain signal by solving an atomic norm minimization problem (an SDP problem). The sample size is $\mathcal{O}(\log N)$, and the off-grid algorithm still allows the samples to be noisy. To recover the frequency support from the output of the off-grid algorithm, we apply the multiple signal classification (MUSIC) algorithm [27]. Although numerically our algorithm for QEEP is very promising, we are unable to prove it satisfies the Heisenberg limit at this moment and will leave it for future work.

The rest part of this paper is organized as follows. We start with preliminaries about QEEP and compressed sensing in Sec. 2. Then we introduce our algorithm that utilizes compressed sensing for QPE in Sec. 3. We also prove the effectiveness of the algorithm and numerically demonstrate its ability. In Sec. 4 we combine off-grid compressed sensing with MUSIC to solve the more generic task of QEEP. We provide a proof of concept numerical demonstration for this method as well. Finally, we summarize several open problems and potential future research directions in Sec. 5.

2 Preliminaries

The notations frequently used in the main text are summarized in Table 1.

Table 1: Notations used in the main text

Notation	Meaning
$y(t)$	sampled time-domain signal
$y^0(t)$	ideal time-domain signal
$z(t)$	noise
$x(k)$	ideal frequency-domain signal
Ω	set of sampled times
ϵ	accuracy of the algorithm
δ	failure probability
η	noise tolerance for each signal

2.1 QEEP as a signal recovery problem

In this section, we express the QEEP as a sparse signal recovery problem and treat QPE as a special case of QEEP. The ideal signal in time domain is

$$y^0(t) = \sum_{f \in \mathcal{F}} c_f e^{-i2\pi ft}, \quad (1)$$

where $c_f \in [0, 1]$, $\sum_f c_f = 1$, and \mathcal{F} is the set of frequency support with $f \in [0, 1]$. When $|\mathcal{F}| = 1$, the problem becomes QPE. The same signal in frequency domain has expression

$$x(k) = \sum_{f \in \mathcal{F}} c_f \delta(k - f). \quad (2)$$

When t and k take values on a discrete set, we use the shorter notations y_k^0 and x_k instead.

Choose a set of times denoted by Ω . For each time $t \in \Omega$, data can be obtained from averaging over the Hadamard tests. More precisely, when $\mathbf{W} = I$, the measurement outcome in Fig. 1 is a random variable

$$h_x(t) = \begin{cases} +1, & p = \frac{1}{2}(1 + \text{Re}(y^0(t))), \\ -1, & p = \frac{1}{2}(1 - \text{Re}(y^0(t))). \end{cases} \quad (3)$$

Similarly, when $\mathbf{W} = S^\dagger$, we obtain

$$h_y(t) = \begin{cases} +1, & p = \frac{1}{2}(1 + \text{Im}(y^0(t))), \\ -1, & p = \frac{1}{2}(1 - \text{Im}(y^0(t))). \end{cases} \quad (4)$$

The summation of the two gives the estimate of $y^0(t)$:

$$E[h(t)] = E[h_x(t) + ih_y(t)] = y^0(t). \quad (5)$$

The task of a QEEP algorithm is to estimate \mathcal{F} with accuracy ϵ by using the data $\{(t, h(t)), t \in \Omega\}$. In other words, assuming the output of the algorithm is \mathcal{F}^* , we require $|\mathcal{F}| = |\mathcal{F}^*|$, and

$$\forall f \in \mathcal{F}, \quad \min_{f^* \in \mathcal{F}^*} |f - f^*| \leq \epsilon. \quad (6)$$

In quantum simulation, the circuit complexity of obtaining a sample of $h(t)$ scales linearly in the evolution time $|t|$ [14] (t can be negative), thus the total experiment cost can be captured by the total runtime, which is defined as

$$T_{\text{total}} = \sum_{t \in \Omega} M(t) \times |t|, \quad (7)$$

where $M(t)$ is the number of repetitions for each t . The Heisenberg limiting scaling could be phrased as satisfying the following:

$$T_{\text{total}} = \mathcal{O}(\epsilon^{-1} \text{poly log}(\epsilon^{-1})). \quad (8)$$

Another important quantity is the maximal runtime $T_{\text{max}} = \max_{t \in \Omega} |t|$, which reflects the maximum circuit depth and is particularly important for early fault-tolerant quantum computers.

One common strategy is, for each time t , we sample the random variable $h(t)$ for M times to obtain a noisy signal at time t :

$$y(t) = \overline{h(t)} = y^0(t) + z(t), \quad (9)$$

then use the noisy samples to recover the frequencies. Here $z(t)$ originates from the statistical uncertainty of the Hadamard tests. Hoeffding's inequality ensures that with probability $1 - \delta'$, we have

$$|z(t)| \leq \mathcal{O}\left(\sqrt{\frac{1}{M} \log \frac{1}{\delta'}}\right). \quad (10)$$

In the rest of the paper, the meanings of $z(t)$ are not identical, but they always represent the part of the signal that should be considered as noise. Introduce the noise tolerance parameter η such that the signal recovery algorithm succeeds as long as the noise of each signal is not larger than η . Thus, to guarantee $|z(t)| < \eta$ for every $t \in \Omega$ with probability $1 - \delta$, we require $\delta \leq \mathcal{O}(\delta' |\Omega|^{-1})$, which implies that M would be proportional to $\mathcal{O}(\log(|\Omega|/\delta)/\eta^2)$ (For a rigorous proof of this see Appendix A of [11]). Now the total runtime is

$$T_{\text{total}} = M \cdot \sum_{t \in \Omega} |t| = \mathcal{O}\left(\log(|\Omega|/\delta) \cdot \eta^{-2} \cdot \sum_{t \in \Omega} |t|\right). \quad (11)$$

For instance, if the algorithm has parameters $M = \mathcal{O}(\log(\epsilon^{-1}))$, $\max |t| = \mathcal{O}(\epsilon^{-1})$, and $|\Omega| = \mathcal{O}(\text{poly log}(\epsilon^{-1}))$, then it achieves the Heisenberg limit. We will see that the algorithm we have using compressed sensing fits this description and hence satisfies the Heisenberg limit.

Let us denote the set of integers from 1 to N as $[N]$. Throughout the paper, if the frequency f satisfies

$$\exists n \in [N], \quad f = n/N, \quad (12)$$

then we say f is on-grid, otherwise it is off-grid. Moreover, for a frequency $f \in [0, 1)$, we define its off-grid deviation as

$$v = \min_{n \in \mathbb{Z}} |f - n/N|. \quad (13)$$

For QEEP, a few set-ups should be added. First, the unitaries U are evolution operators under Hamiltonian H for different evolution times. To keep the notations consistent, we still regard t as a dimensionless integer and introduce a fixed time step τ so that the actual evolution times are $\{t\tau, t \in \Omega\}$. Given a specific Hamiltonian with energy eigen basis $H = \sum_{\ell} E_{\ell} P_{\ell}$ and an initial state ρ , the time domain signal in QEEP could be written as

$$y^0(t) = \text{tr}(e^{-iHt\tau} \rho) = \sum_{\ell} \text{tr}(P_{\ell} \rho) e^{-iE_{\ell}\tau t}. \quad (14)$$

Thus, \mathcal{F} has a linear relation with the set of energy levels $\{E_{\ell}\}$ that have non-zero overlaps with the initial state ρ :

$$\mathcal{F} = \{E_{\ell}\tau/2\pi : \text{tr}(P_{\ell}\rho) > 0\}. \quad (15)$$

Note that the frequencies are defined on $[0, 1)$. To keep the order of energy levels unchanged, it is necessary to assume

$$\forall \ell, \quad E_\ell \tau \in [0, 2\pi), \quad (16)$$

which can always be satisfied by adding a constant term to H and choosing τ properly.

For the special case of QPE, without loss of generality, we will be mainly discussing the estimation of the ground energy, i.e., the smallest eigenvalue of H . In general, we do not expect to be able to prepare the exact ground state but assume the initial state has a large overlap with the ground state:

$$|\Phi\rangle = \sqrt{1-\gamma}|\Psi\rangle + \sqrt{\gamma}|\Psi^\perp\rangle. \quad (17)$$

The γ here is equivalent to $1 - p_0$ in the introduction. As long as γ is smaller than a small constant, the signal is still dominated by $e^{-iE_0 t}$, and the ground energy E_0 can be estimated efficiently.

2.2 Compressed sensing

In this section we introduce necessary concepts and notations for compressed sensing. Given a vector $v = [v_1, v_2, \dots, v_N]^\top$, its 1-norm, 2-norm, and ∞ -norm are defined as

$$\|v\|_1 = \sum_{n=1}^N |v_n|, \quad \|v\|_2 = \left(\sum_{n=1}^N |v_n|^2 \right)^{1/2}, \quad \|v\|_\infty = \max_n |v_n|. \quad (18)$$

The ideal time domain signal y^0 can be written as an N -dimensional vector

$$y^0 = [y_1^0, y_2^0, \dots, y_N^0]^\top. \quad (19)$$

Let us define the Fourier matrix as $F_{kt} = e^{-i2\pi kt/N}$, $k, t \in [N]$. By labeling its columns with $\{w_t, t \in [N]\}$,

$$F = [w_1, w_2, \dots, w_N]. \quad (20)$$

If all $f \in \mathcal{F}$ are on-grid satisfying Eq. (12), the frequency-domain signal x can be written in the form of a vector as

$$x = \frac{1}{N} F^\dagger y^0, \quad y^0 = Fx. \quad (21)$$

If $y_t^0 = \sum_{f \in \mathcal{F}} c_f e^{-i2\pi ft}$, then $x_k = \sum_{f \in \mathcal{F}} c_f \delta_{k, Nf}$ is a sparse vector with $|\mathcal{F}|$ non-zero entries.

Now consider sampling $|\Omega|$ elements from $[N]$ as a collection of evolution times: $\Omega = \{t_1, t_2, \dots, t_{|\Omega|}\}$. Based on the choice of Ω , we define the partial inverse Fourier transformation and the signal samples as

$$F_\Omega = [w_{t_1}, w_{t_2}, \dots, w_{t_{|\Omega|}}], \quad (22)$$

$$y_\Omega^0 = [y_{t_1}^0, y_{t_2}^0, \dots, y_{t_{|\Omega|}}^0]^\top. \quad (23)$$

With these notations, the compressed sensing algorithm can be thought as solving the optimization problem

$$\min \|s\|_1, \quad s.t. \quad F_\Omega s = y_\Omega^0. \quad (24)$$

When the frequency support \mathcal{F} is sparse in the sense that $|\mathcal{F}| \leq \mathcal{O}(\log N)$, the optimal solution $s^\#$ equals to the frequency-domain signal x with high probability. Rigorous statements can be found in [20].

Moreover, provided that the signal has extra noise $y_t = y_t^0 + z_t$, where $|z_t| \leq \eta$, the signal can be approximately recovered by the convex relaxation algorithm [21]:

$$\min \|s\|_1, \quad s.t. \quad \|F_\Omega s - y_\Omega\|_2 \leq \sqrt{|\Omega|}\eta. \quad (25)$$

The difference between $s^\#$ and x depends on the size of η .

The uniqueness and robustness of compressed sensing solution can be analyzed through the so-called dual certificate [22]. In optimization, the dual certificate is the optimal solution to the dual problem. In a regular compressed sensing task where all frequencies are on-grid, for each frequency support \mathcal{F} and each sample set Ω , the dual certificate is an N -dimensional vector p such that

$$\exists V, \quad p = F_\Omega^\dagger V, \quad (26)$$

$$\forall k/N \in \mathcal{F}, \quad p_k = 1, \quad (27)$$

$$\forall k/N \notin \mathcal{F}, \quad |p_k| < 1 - \varepsilon(\Omega), \quad (28)$$

where $\varepsilon(\Omega) \in (0, 1)$ is determined by the size of Ω . The existence of such a dual certificate is called the exact reconstruction principle [20]. Using dual certificate as a pivot, we can quantify the part of $s^\#$ that is not supported on \mathcal{F} , which further helps us determine the accuracy of the algorithm. The basic idea is to separate the entries of $s^\#$ into two parts:

$$\sum_{k/N \in \mathcal{F}} |s_k^\#|, \quad \sum_{k/N \notin \mathcal{F}} |s_k^\#|. \quad (29)$$

Because the true frequency-domain solution x_k satisfies the constraint in Eq. (25), the 1-norm of $s^\#$ is upper bounded by the 1-norm of x . On the other hand, the norm of the inner product between $s^\#$ and p can be well-estimated, and the restrictions on the entries of p enable us to deal with $\sum_{k/N \in \mathcal{F}} |s_k^\#|$ and $\sum_{k/N \notin \mathcal{F}} |s_k^\#|$ separately. The combination of these considerations eventually provides us an upper bound on $\sum_{k/N \notin \mathcal{F}} |s_k^\#|$ as we will see later.

3 Single eigenvalue estimation with on-grid compressed sensing

In this section, we first provide a quantitative restriction on the noise tolerance η in Eq. (25). Then by considering the combination of three sources of inexactness namely, the uncertainty of the Hadamard test, the inaccuracy of the initial state, and the off-grid deviation, as noise, we prove performance bounds for our algorithm.

Let us consider the case when the signal contains only one frequency $\mathcal{F} = \{f\}$ and the frequency is on-grid: $f = n/N$, for which we are given the values of

$$y_t^0 = e^{-i2\pi nt/N} \quad (30)$$

on random sample set Ω . Notice that the frequency-domain signal is $x_k = \delta_{k,n}$. The following lemma shows how its dual certificate can be constructed.

Lemma 1. *Given the values of signal $y_t^0 = e^{-i2\pi nt/N}$ on a random sample set Ω with size larger than $\mathcal{O}(\log(N/\delta)/(1 - \varepsilon)^2)$, the random vector $p = F_\Omega y_\Omega^0 / |\Omega|$ satisfies*

$$p_n = 1, \quad |p_k| \leq 1 - \varepsilon, \quad k \neq n \quad (31)$$

with probability at least $1 - \delta$.

Proof. See Appendix 7.1. \square

We can thus prove the robust recovery of Eq. (25) with the properties of dual certificate p .

Lemma 2. *Given a noisy signal $y_t = e^{-i2\pi nt/N} + z_t$ and a random sample Ω with size $\lceil 32 \ln(4(N-1)/\delta)/3 \rceil$. If the noise satisfies $\|z_\Omega\|_2 \leq \sqrt{|\Omega|}\eta$, the solution $s^\#$ to Eq. (25) satisfies:*

$$\sum_{k \neq n} |s_k^\#| \leq 4\eta, \quad |s_n^\#| \geq 1 - 4\eta. \quad (32)$$

with probability at least $1 - \delta$.

Proof. See Appendix 7.2. \square

By Lemma 2 we see that as long as $\eta < 1/8$, we have $|s_n^\#| > \sum_{k \neq n} |s_k^\#|$, so the solution to Eq. (25) still satisfies $n = \arg \max s_k^\#$. The result means the noise tolerance of each signal is independent of N .

In practical situations we cannot assume that the frequency is always perfectly on-grid, but this should not cause a serious problem. Intuitively, as long as the off-grid deviation is small enough, that should not make a difference where we are handling the noisy signals in Lemma 2. By treating the deviation in frequency as noise, we can verify this intuition and also estimate how large the off-grid deviation can be.

Proposition 1. *Given a signal $y_t = e^{-i2\pi(n+\omega)t/N}$ with $n \in \mathbb{Z}_N$, $\omega \in (-0.5, 0.5]$ and a set of samples Ω with size $|\Omega| \geq \lceil 32 \ln(4(N-1)/\delta)/3 \rceil$, if $|\omega| < 1/16\pi$, then with probability at least $1 - \delta$, the optimal solution $s^\#$ to Eq. (24) satisfies*

$$n = \arg \max s_k^\#. \quad (33)$$

Proof. In this situation, we have

$$z_t = y_t(e^{i2\pi vt/N} - 1), \quad |z_t| = 2|\sin(\pi\omega t/N)| < 2\pi\omega t/N. \quad (34)$$

According to Lemma 2, one sufficient condition for robust recovery is $|z_t| \leq 1/8$ for all t . Hence it is enough to have $|\omega| \leq 1/16\pi$. \square

The $|\omega|$ in Proposition 1 represents the off-grid deviation. If $|\omega| \leq 1/16\pi$, the solution $f^\# = \arg \max s_k^\#/N$ is still a good approximation of $(n + \omega)/N$, and the accuracy still scales as $\mathcal{O}(N^{-1})$. When the off-grid deviation is large, we can find a grid-shift parameter ν such that after the transformation $y_t \rightarrow y_t e^{i2\pi\nu t/N}$, the new signal is nearly on-grid. The details are in Algorithm 1.

Besides the Hadamard tests and the off-grid deviation, the third type of noise comes from the preparation of initial state. In practice, it is hard to prepare the exact ground state $|\Psi\rangle$. Suppose the actual initial state is

$$|\Phi\rangle = \sqrt{1-\gamma}|\Psi\rangle + \sqrt{\gamma}|\Psi^\perp\rangle. \quad (35)$$

Then y_t^0 can be expanded as

$$\langle \Phi | U(t) | \Phi \rangle = e^{-iE_0 t} + \sqrt{\gamma(1-\gamma)}(\langle \Phi | U(t) | \Phi^\perp \rangle + c.c) + \mathcal{O}(\gamma). \quad (36)$$

Only $e^{-iE_{\text{tot}}t}$ is the target signal and we can treat the $\mathcal{O}(\sqrt{\gamma})$ term as noise as well. Recall that in Lemma 2, as long as $\eta < 1/8$, the noise does not break down the signal recovery. We separate η into three parts. Let η_1 denote the inaccuracy of the initial state preparation, η_2 of the Hadamard tests, and η_3 of the grid shift. As long as $\eta_1^2 + \eta_2^2 + \eta_3^2 \leq 1/64$, the signal recovery is robust.

Given the values of η_1, η_2, η_3 , the overlap γ with $2\sqrt{\gamma} \leq \eta_1$, the number of Hadamard tests that is at least $\mathcal{O}(\log|\Omega|/\eta_2^2)$, and the number of grid shifts as $\lceil 2\pi/\eta_3 \rceil$, the algorithm for QPE is given in Algorithm 1.

Algorithm 1 Single eigenvalue estimation (QPE)

Input: accuracy level N , time step τ , failure probability δ_1, δ_2 , noise tolerance η_1, η_2, η_3 , Hamiltonian H , and initial state $|\Phi\rangle$ with overlap larger than $\sqrt{1 - \eta_1^2/4}$.

Output: $E^* = 2\pi k^*/N$.

- 1: Sample a set of $\lceil 32 \ln(8\pi(N-1)/\delta_1\eta_3)/3 \rceil$ random integers from $[N]$, denoted by Ω .
- 2: **for** $t \in \Omega$ **do**
- 3: Prepare the approximated ground state and unitary operator $e^{-iHt\tau}$;
- 4: Perform Hadamard tests on $e^{-iHt\tau}|\Phi\rangle$ for $\mathcal{O}(\log(|\Omega|/\delta_2)/\eta_2^2)$ times;
- 5: Calculate the average value of the test outcomes as signal y_t .
- 6: **end for**
- 7: **for** $j = 1, 2, \dots, \lceil 2\pi/\eta_3 \rceil$ **do**
- 8: Set $\nu = -0.5 + j/\lceil 2\pi/\eta_3 \rceil$;
- 9: Generate a new signal set $\tilde{y}_t = y_t \cdot e^{i2\pi t\nu/N}$;
- 10: Set $\eta = \sqrt{\eta_1^2 + \eta_2^2 + \eta_3^2}$. Solve Eq. (25) with \tilde{y}_Ω and obtain solution $s^\#$;
- 11: Set $\tilde{k}_\nu = \arg \max_k s_k^\# + \nu$;
- 12: Calculate the total empirical error $\sum_{t \in \Omega} |y_t - e^{-i2\pi \tilde{k}_\nu t/N}|^2$. Only keep all the \tilde{k}_ν with total empirical error smaller than $|\Omega|(\eta_1^2 + \eta_2^2 + \eta_3^2)$;
- 13: **end for**
- 14: Find the frequency \tilde{k}_ν with the smallest total empirical error, set it as k^* .

Theorem 1. *Given the ground state $|\Psi\rangle$, the ground-state energy E_0 , and the initial state $|\Phi\rangle = \sqrt{1-\gamma}|\Psi\rangle + \sqrt{\gamma}|\Psi^\perp\rangle$, if the noise tolerance parameters satisfy*

$$\eta_1^2 + \eta_2^2 + \eta_3^2 \leq \frac{1}{64}, \quad \eta_1 \geq 2\sqrt{\gamma}, \quad (37)$$

then with probability at least $(1 - \delta_1)(1 - \delta_2)(1 - \delta_3)$, $\delta_3 < 2 \exp(-|\Omega|/9)$, the output of Algorithm 1 satisfies

$$|E_0 - E^*| \leq \max \left\{ \frac{\eta_3}{N\tau}, \frac{8\sqrt{3\eta_1^2 + 3\eta_2^2}}{N\tau} \right\} = \frac{2\pi\epsilon}{\tau}, \quad (38)$$

and the cost of the algorithm satisfies

$$T_{\max} \leq N\tau, \quad (39)$$

$$T_{\text{total}} = \mathcal{O} \left(N\tau \cdot \log(N/\delta_1\eta_3) \cdot \log(\log(N/\delta_1\eta_3)/\delta_2)/\eta_2^2 \right). \quad (40)$$

Proof. In the algorithm, δ_1 is the total failure rate of compressed sensing algorithms, δ_2 is the total failure rate of Hadamard tests. Therefore, $\lceil 32 \ln(8\pi(N-1)/\delta_1\eta_3)/3 \rceil$ number of samples ensures that all compressed sensing algorithms succeed with probability $1 - \delta_1$; and $(\log(|\Omega|\delta_2^{-1})/\eta_2^2)$ Hadamard tests are enough to guarantee that for all t , the additive error from the Hadamard tests is smaller than η_2 with probability $1 - \delta_1$.

Now we intend to determine the accuracy on E_0 . Let $k_0 = NE_0\tau/2\pi = n + \omega$. The choice of the set of grid shift parameters ensures that there must exist at least one $\tilde{k}_\nu = n + \nu$ satisfying $|\nu - \omega| < \eta_3/2\pi$. Furthermore, the restriction $\sum_{t \in \Omega} |y_t - e^{-i2\pi\tilde{k}_\nu t/N}|^2 \leq |\Omega|(\eta_1^2 + \eta_2^2 + \eta_3^2)$ ensures that the qualified \tilde{k}_ν must belong to region

$$\left(k_0 - \frac{\sqrt{\eta_3^2 + 2\eta_1^2 + 2\eta_2^2}}{2\pi}, k_0 + \frac{\sqrt{\eta_3^2 + 2\eta_1^2 + 2\eta_2^2}}{2\pi} \right). \quad (41)$$

Combining it with the upper bound $\eta_1^2 + \eta_2^2 + \eta_3^2 \leq 1/64$, we can limit our attention to the following function

$$\mathcal{E}(k, k_0) = \sum_{t \in \Omega} \left| e^{-i2\pi k_0 t/N} - e^{-i2\pi k t/N} + z_t \right|^2, \quad k \in (k_0 - 1/8\pi, k_0 + 1/8\pi). \quad (42)$$

Here z_t is the error caused by the Hadamard tests and the initial state preparation, with $|z_t| \leq \bar{\eta} = \sqrt{\eta_1^2 + \eta_2^2} < 1/8$. Hence,

$$\mathcal{E}(k, k_0) - \sum_{t \in \Omega} \left| e^{-i2\pi k t/N} - e^{-i2\pi k_0 t/N} \right|^2 \in [-|\Omega|\bar{\eta}^2, |\Omega|\bar{\eta}^2]. \quad (43)$$

If we define a random variable $Y_t = |e^{i2\theta t} - 1|^2$ with $\theta = \pi(k - k_0)/N$, since $t\theta \in (-1/8, 1/8)$ and $x/2 \leq |\sin x| \leq x$ holds inside this region, we have

$$\theta^2 \sum_{t \in \Omega} t^2 \leq \sum_{t \in \Omega} Y_t \leq 4\theta^2 \sum_{t \in \Omega} t^2, \quad (44)$$

$$E[t^2] = \frac{1}{6}(N+1)(2N+1) \approx \frac{N^2}{3}. \quad (45)$$

Using Hoeffding's inequality, we obtain

$$P \left[\left| \sum_{t \in \Omega} t^2 - |\Omega|E[t^2] \right| > s \right] \leq 2 \exp \left(-\frac{2s^2}{|\Omega|(N^2 - 1)^2} \right). \quad (46)$$

By choosing $s = |\Omega|E[t^2]/2$, we show that with probability at least $1 - 2 \exp(-|\Omega|/9)$ we have

$$\sum_{t \in \Omega} t^2 \in \left(\frac{1}{2}|\Omega|E[t^2], \frac{3}{2}|\Omega|E[t^2] \right), \quad (47)$$

$$\sum_{t \in \Omega} \left| e^{-i2\pi k t/N} - e^{-i2\pi k_0 t/N} \right|^2 = \alpha |\Omega|\pi^2 |k - k_0|^2, \quad \alpha \in (1/6, 2). \quad (48)$$

Therefore, the k^* that minimizes $\mathcal{E}(k, k_0)$ must be in the region

$$\left(k_0 - \frac{2\sqrt{3}\bar{\eta}}{\pi}, k_0 + \frac{2\sqrt{3}\bar{\eta}}{\pi} \right). \quad (49)$$

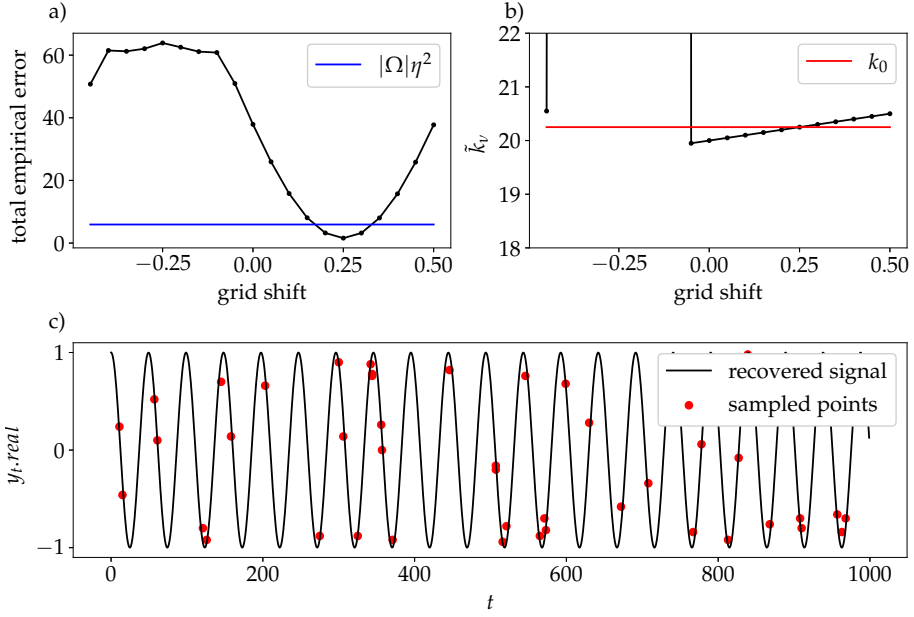


Figure 2: Searching for the optimal grid shift parameter. Set $N = 1000$, $|\Omega| = 50$, and $\eta = 0.344$. In this numerical test, the noiseless signal is $0.9e^{-i2\pi f_0 t} + 0.1e^{-i2\pi f_1 t}$ with $f_0 = 0.02025$ and $f_1 = 0.1$. Each noisy signal is sampled from $M = 100$ Hadamard tests. The set of grid shift parameters is $\{-0.5 + j/20\}$. As shown by Fig a), the grid shift parameter that minimizes the total empirical error is exactly $\nu = 0.25$. Only three \tilde{k}_ν s are qualified. Fig b) shows the value \tilde{k}_ν as a function of the grid shift parameter ν . Here $k_0 = 20.25$ is linked to the target frequency f_0 . Fig c) shows the comparison between the sampled data and the recovered data.

Assuming $\eta_3/2\pi < 4\sqrt{3}\bar{\eta}/\pi$, there must exist at least one \tilde{k}_ν in this region, so the accuracy of k^* is $4\sqrt{3}\bar{\eta}/\pi$; otherwise the accuracy of the algorithm is determined by η_3 only. Thus, the final accuracy of the algorithm is

$$\frac{2\pi}{N\tau} \times \max \left\{ \frac{\eta_3}{2\pi}, \frac{4\sqrt{3}\sqrt{\eta_1^2 + \eta_2^2}}{\pi} \right\}. \quad (50)$$

The maximal runtime equals to $\max_{t \in \Omega} |t| \times \tau$. Because Ω is sampled from $[N]$, we have $T_{\max} \leq N\tau$. The upper bound on T_{total} can be obtained from Eq. (11) and related parameters in the algorithm. \square

In Fig. 2 we demonstrate our algorithm with a simple test case where the target frequency is $f_0 = (n + \omega)/N$ with $N = 1000$, $n = 20$ and $\omega = 0.25$. As shown by the Figure, when the grid shift parameter is in region $[0, 0.5]$, the integer parts of $\{\tilde{k}_\nu\}$ are all 20, which matches with the true frequency. In the same region, the total empirical error is approximately a quadratic function of the grid shift parameter.

For this test, the three noise tolerance parameters are

$$\eta_1 = 0.1, \quad \eta_2 \approx 0.1, \quad \eta_3 = \frac{\pi}{10}, \quad (51)$$

therefore $\eta \approx 0.344$. Clearly, the noise tolerance parameters do not satisfy Eq. (37), but the algorithm still outputs the true frequency $f^* = 0.02025$. This numerical experiment demonstrates that the parameters in Lemma 2 and Theorem 1 can be further improved.

Unfortunately this method does not work for the multiple eigenvalue estimation because we cannot guarantee that all the frequencies in \mathcal{F} are nearly on-grid. For example, if

$f_0 = n_0/N, f_1 = (n_1 + 0.5)/N$, the compressed sensing algorithm is not guaranteed to work no matter how we choose the grid shift parameter. In the next section we discuss a potential way to solve the QEEP by another type of compressed sensing algorithm instead.

4 Multiple eigenvalue estimation with off-grid compressed sensing

In this section we discuss an off-grid compressed sensing algorithm for multiple eigenvalue estimation. Although the algorithm we will be describing works well numerically, its rigorous proof of the Heisenberg limit is hard, which we will leave it for future work.

For the on-grid compressed sensing, Eq. (24) can be written in the following concise form:

$$\min \|Fr\|_1, \quad s.t. \quad r_\Omega = y_\Omega, \quad (52)$$

where r is the inverse Fourier transformation of the original ansatz s . The idea of off-grid compressed sensing is similar, except we need to introduce another norm for the continuous values of frequencies [25]:

$$\min \|r\|_{\mathcal{A}}, \quad s.t. \quad r_\Omega = y_\Omega, \quad (53)$$

$$\|r\|_{\mathcal{A}} = \inf_{c_f \geq 0, \phi_f \in [0, 2\pi), f \in [0, 1)} \left\{ \sum_f c_f : r_t = \sum_f c_f e^{i(2\pi f t + \phi_f)} \right\}. \quad (54)$$

The new vector norm $\|\cdot\|_{\mathcal{A}}$ is called the atomic norm, which can be written as the solution of a semidefinite programming (SDP) problem (see Proposition 2.1 of [25]):

$$\|r\|_{\mathcal{A}} = \inf_{u, v} \left\{ \frac{1}{2N} \text{tr}(\text{Toep}(u)) + \frac{v}{2} : \begin{bmatrix} \text{Toep}(u) & r \\ r^\dagger & v \end{bmatrix} \succeq 0 \right\}, \quad (55)$$

where u is an $2N + 1$ -dimensional vector (in the off-grid case, instead of choosing t from $[N]$, we allow it to take values from $-N$ to N), v is a real number, and $\text{Toep}(u)$ represents a Toeplitz matrix whose first column is u :

$$(\text{Toep}(u))_{mn} = u_{m-n}, \quad u_{-n} = u_n^\dagger. \quad (56)$$

Thus, the full optimization task for off-grid compressed sensing is

$$\min_{u, r, v} \frac{1}{2N} \text{tr}(\text{Toep}(u)) + \frac{v}{2}, \quad s.t. \quad \begin{bmatrix} \text{Toep}(u) & r \\ r^\dagger & v \end{bmatrix} \succeq 0, \quad r_\Omega = y_\Omega. \quad (57)$$

Suppose the error tolerance for each signal is η , then the robust version that allows small noise is given as

$$\min_{u, r, v} \frac{1}{2} \|r_\Omega - y_\Omega\|_2^2 + \lambda \left(\frac{1}{2N} \text{tr}(\text{Toep}(u)) + \frac{v}{2} \right), \quad s.t. \quad \begin{bmatrix} \text{Toep}(u) & r \\ r^\dagger & v \end{bmatrix} \succeq 0, \quad (58)$$

with $\lambda = \Theta(\eta \sqrt{|\Omega|/|\mathcal{F}|})$. This is the so-called Beurling-Lasso algorithm [28].

The next theorem is simply a rewriting of the result of [26] with our notations.

Theorem 2. *Suppose we have the signal*

$$y_t = y_t^0 + z_t, \quad y_t^0 = \sum_{f \in \mathcal{F}} c_f e^{i2\pi f t}, \quad t = -N, -N+1, \dots, N, \quad (59)$$

where c_f are positive numbers with summation 1, $f \in [0, 1)$. We know the value of y_t on random sample set Ω . The the solution to Eq. (58) is $r_t^\#$, $t = -N, -N+1, \dots, N$, which can be decomposed as

$$r_t^\# = \sum_{g \in \mathcal{G}} d_g e^{i2\pi gt}. \quad (60)$$

To quantify the similarity between \mathcal{G} and \mathcal{F} , define

$$\Delta_{\mathcal{F}} = \min_{n \in \mathbb{Z}} \min_{f_1 \neq f_2 \in \mathcal{F}} |f_1 - f_2 + n|, \quad (61)$$

$$R_f^{near} = \left\{ k : \frac{\pi^2}{3} N(N+4)(k-f)^2 \leq \frac{1}{128} \right\}, \quad (62)$$

$$R_f^{far} = [0, 1) \setminus \bigcup_{f \in \mathcal{F}} R_f^{near}. \quad (63)$$

Then the estimator for f is

$$\hat{f} = \text{average value of } \{g : g \in R_f^{near}\}, \quad (64)$$

and the estimator for c_f as

$$\hat{c}_f = \sum_{g \in R_f^{near}} d_g. \quad (65)$$

If $N \geq 128$, $\|z_\Omega\|_2 \leq \sqrt{|\Omega|}\eta$, $\Delta_{\mathcal{F}} > \frac{2|\mathcal{F}|^{1/4}}{\sqrt{N(N+4)}}$, $\lambda = \Theta(\eta\sqrt{|\Omega|/|\mathcal{F}|})$, and

$$|\Omega| \geq \mathcal{O} \left(\max \left\{ |\mathcal{F}| \log \frac{N}{\delta}, |\mathcal{F}| \log^2 \frac{|\mathcal{F}|}{\delta} \right\} \right), \quad (66)$$

introduce a constant $\varepsilon_0 \approx 0.000504$, then we have

$$|\hat{c}_f - c_f| \leq 8\sqrt{|\Omega|}\eta + (8\lambda + \sqrt{|\Omega|}\eta)\sqrt{|\mathcal{F}|} + 4\lambda + \frac{1 - \varepsilon_0}{\varepsilon_0} \frac{(\sqrt{|\Omega|}\eta + \lambda\sqrt{|\mathcal{F}|})^2}{2\lambda}, \quad (67)$$

$$|\hat{f} - f| \leq \frac{1}{8\sqrt{6}N}, \quad \sum_{g \in R_f^{far}} |d_g| \leq \frac{(\sqrt{|\Omega|}\eta + \lambda\sqrt{|\mathcal{F}|})^2}{2\varepsilon_0\lambda} \quad (68)$$

with probability at least $1 - \delta$.

The more detailed discussions can be found in Proposition 1, Proposition 2, and Appendix C of [26]. Roughly speaking, similarly to the regular compressed sensing, $\mathcal{O}(\log N)$ random samples are enough to approximately recover the noisy signal. But the output of off-grid compressed sensing $r_t^\#$ is an estimate for the time domain signal, not the frequency domain signal. We need an extra step to recover the frequency support. In signal recovery, when the minimal frequency gap of the signal has lower bound N^{-1} , we say the frequency support is well-separated and can be recovered easily. However, we do not have any conclusion about the minimal frequency gap of the output signal $r_t^\#$, thus the original method in [25] that depends on the reconstruction of dual certificate is not guaranteed to work. Besides, in practice the performance of the original algorithm is very sensitive to noise, which makes it impractical. We need a different post-processing procedure to recover an estimation of \mathcal{F} from $r^\#$.

The multiple signal classification (MUSIC) algorithm [27] is one strong candidate. This algorithm is constructed on the Hankel matrix that is defined as (when t takes value from $-N$ to N)

$$(\text{Hank}(y))_{mn} = y_{m+n-N-1}, \quad m, n \in [N]. \quad (69)$$

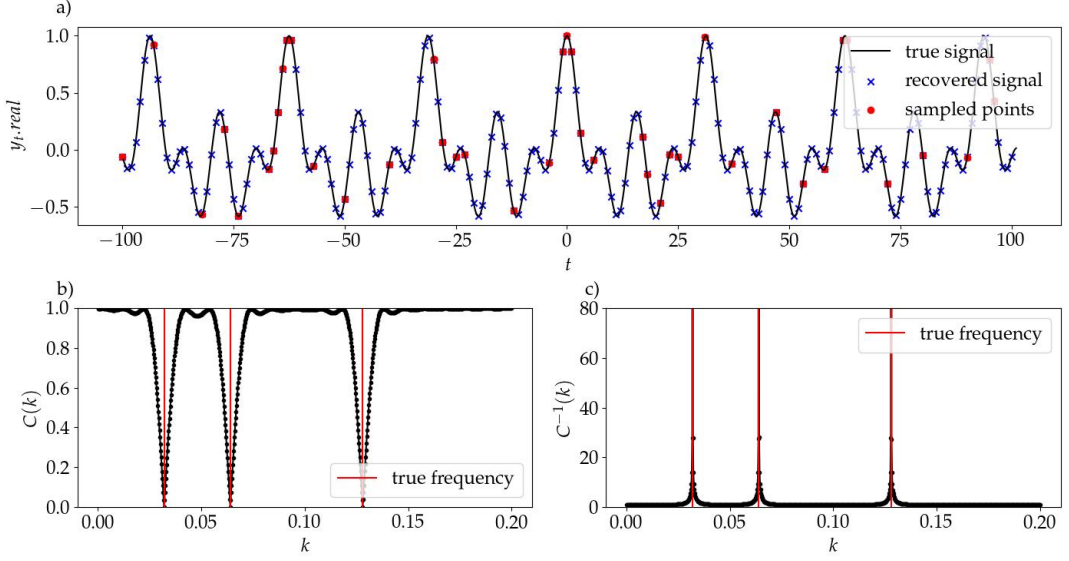


Figure 3: Signal recovery by off-grid compressed sensing and MUSIC algorithm. The example uses signal $y_t^0 = \frac{1}{3}e^{-i2\pi f_1 t} + \frac{1}{3}e^{-i2\pi f_1 t} + \frac{1}{3}e^{-i2\pi f_3 t}$ with $f_1 = 0.032$, $f_2 = 0.064$, and $f_3 = 0.128$. We set $N = 100$ (totally 201 points), $|\Omega| = 50$, and $\lambda = 0.05$. The sampled data comes from taking the average over 500 Hadamard tests. Fig a) shows the comparison between the real parts of the true signal y^0 , the sampled signal y_Ω , and the recovered signal from the off-grid compressed sensing $r^\#$. Fig b) shows the outcomes of the MUSIC algorithm. The local minima of $C(k)$ are the estimators of \mathcal{F} . Fig c) shows the inverse of $C(k)$.

For a noisy signal $y_t = y_t^0 + z_t$, we can further separate the Hankel matrix into two parts:

$$\text{Hank}(y) = \text{Hank}(y^0) + \text{Hank}(z). \quad (70)$$

The Hankel matrix has the following decomposition:

$$\text{Hank}(y^0) = \sum_{f \in \mathcal{F}} c_f e^{-i2\pi(N-1)f} a(f)^\top a(f), \quad (71)$$

$$a(k) = [e^{i2\pi k} \ e^{i2\pi 2k} \ \dots \ e^{i2\pi Nk}]^\top. \quad (72)$$

Therefore, the set of $\{a(f), f \in \mathcal{F}\}$ can be found in the space spanned by the vectors with the $|\mathcal{F}|$ largest singular values of $\text{Hank}(y^0)$. Define the projector onto the null space of $\text{Hank}(y^0)$ as P_{null} . Define the noise-space correlation function as

$$C_0(k) = \frac{\|P_{\text{null}}a(k)\|_2}{\|a(k)\|_2}. \quad (73)$$

It turns out $C_0(k) = 0$ if and only if $k \in \mathcal{F}$ (see Theorem 1 of [27]). Similarly, we can define $C(k)$ as the noise-space correlation function for y , and as long as $\text{Hank}(z)$ does not perturb the null space too much, the local minima of $C(k)$ can serve as estimators for \mathcal{F} .

Combining the MUSIC algorithm with the off-grid compressed sensing we obtain Algorithm 2 for the QEEP. A numerical test that demonstrates the efficiency of the algorithm is in Fig. 3.

5 Discussion

In this paper we present two simple and robust algorithms for quantum phase estimation using compressed sensing. The first one is designed for the single eigenvalue estimation

Algorithm 2 Multiple eigenvalue estimation (QEEP)

Input: accuracy level N , time step τ , size of frequency support $|\mathcal{F}|$, expected failure probability δ_1, δ_2 , Hamiltonian H , and an initial state ρ .

Output: the $|\mathcal{F}|$ smallest local minima of $C(k)$.

- 1: Sample $\mathcal{O}\left(\max\left\{|\mathcal{F}|\log(N/\delta_1), |\mathcal{F}|\log^2(|\mathcal{F}|/\delta_1)\right\}\right)$ random integers from $[-N, N]$ as Ω .
- 2: **for** $t \in \Omega$ **do**
- 3: Prepare the initial state ρ and evolution operator $e^{-iHt\tau}$;
- 4: Perform Hadamard tests on $e^{-iHt\tau}\rho e^{iHt\tau}$ for $\mathcal{O}(\log(|\Omega|\delta_2^{-1}))$ times;
- 5: Calculate the average value of the test outcomes as signal y_t .
- 6: **end for**
- 7: Solve Eq. (58) with y_Ω to obtain solution $r^\#$.
- 8: Perform singular value decomposition on $\text{Hank}(r^\#)$:

$$\text{Hank}(r^\#) = [u_1, u_2, \dots, u_{|\mathcal{F}|} \dots] \text{diag}\{\sigma_1, \sigma_2, \dots, \sigma_{|\mathcal{F}|}, \dots\} [v_1, v_2, \dots, v_{|\mathcal{F}|} \dots]^\dagger,$$

where $\{\sigma_1, \sigma_2, \dots, \sigma_{|\mathcal{F}|}\}$ are the $|\mathcal{F}|$ largest singular values.

- 9: Find the projector onto $\text{span}\{u_1, u_2, \dots, u_{|\mathcal{F}|}\}$ as P_1 .
- 10: Compute the noise-space correlation function: $C(k) = \|(I - P_1)a(k)\|_2 / \|a(k)\|_2$.

problem (QPE), which we prove achieves the Heisenberg limit. The second one combines two classical algorithms Beurling-LASSO and MUSIC, which works for the general multiple eigenvalues estimation problem (QEEP) and has the potential to achieve the Heisenberg limit as well.

For QPE, compared to the other two recent work [11, 12], one advantage of our method is the flexibility in choosing the evolution times. In previous algorithms, one needs to prepare unitary operators at times $\{2^j T_{\min}, j = 0, 1, 2 \dots\}$, while our evolution times are homogeneous from T_{\min} to T_{\max} , and the difference between evolution times is not so large. Moreover, even if the sampling of the evolution times is not completely random, the compressed sensing algorithm still succeeds with high probability. This feature can potentially reduce the complexity of the experiments. Besides, the main post-processing step in our algorithms is solving a linear programming problem, which is computationally easier and more stable than the least square minimization in [11].

One drawback of our current algorithm is that we require a much higher initial overlap p_0 compared to the other recent works [7, 11, 12]. This can be potentially avoided in the general framework of QEEP. The intuition is that if the signal has several non-trivial sinusoidal function components, none of them is more special than others, and we should be able to estimate them simultaneously. A more rigorous analysis of Algorithm 2 is needed, which we will leave its full investigation for future work.

Lastly, we summarize a few open questions here:

- As we mentioned along the numerical demonstration in Fig.2, the results suggest robustness of our algorithm beyond what we were able to prove. Thus it should be possible to further improve the noise tolerance in Lemma 2, which would also result in reducing the total runtime in our analysis.
- Instead of sampling discrete times steps, we can also sample the evolution times on a continuous region. Similar to the set up in [18], we can design a probability distribution of evolution times $q(t)$, which then, as long as $E_q[|t|] = \mathcal{O}(N^{-1})$, the

Heisenberg limit is still satisfied. Theoretically, continuous Fourier sampling can further reduce the sample complexity and maximal evolution time.

- Proving or disproving that Algorithm 2 achieves the Heisenberg limit. The result in Theorem 2 is already good in the sense that if we are given the frequency support \mathcal{G} of $r^\#$, we can easily output an estimator for \mathcal{F} with accuracy level $\mathcal{O}(N^{-1})$. However, it is possible to have $g_1, g_2 \in \mathcal{G}$ that are both close to f while $|g_1 - g_2|$ is arbitrarily small. It is in general hard to recover the frequency-domain signal from the time-domain signal in such cases without restrictions in the minimal frequency gap. Thus, the main difficulty is to show that even without the knowledge of the minimal frequency gap, a low resolution solution of frequencies with accuracy level $\mathcal{O}(N^{-1})$ is still possible.
- Combining the off-grid compressed sensing algorithm with subspace methods (e.g., MUSIC and ESPRIT) in a more concise way. For example, the Toeplitz matrix has direct connection with the Hankel matrix representation of the signal, and the Hankel matrix is the starting point of MUSIC and ESPRIT algorithm. Therefore, one can try to directly output the frequencies using the Toeplitz matrix in Eq. (57).

6 Acknowledgement

We thank Tianyu Wang for helpful discussions. C.Y. acknowledges support from the National Natural Science Foundation of China (Grant No. 92165109), National Key Research and Development Program of China (Grant No. 2022YFA1404204), and Shanghai Municipal Science and Technology Major Project (Grant No. 2019SHZDZX01). C.Z. and J.T. acknowledge support from the U.S. National Science Foundation under Grant No. 2116246, the U.S. Department of Energy, Office of Science, National Quantum Information Science Research Centers, and Quantum Systems Accelerator.

References

- [1] A Yu Kitaev. Quantum measurements and the abelian stabilizer problem. *arXiv preprint quant-ph/9511026*, 1995.
- [2] Peter W Shor. Polynomial-time algorithms for prime factorization and discrete logarithms on a quantum computer. *SIAM review*, 41(2):303–332, 1999.
- [3] Daniel S Abrams and Seth Lloyd. Quantum algorithm providing exponential speed increase for finding eigenvalues and eigenvectors. *Physical Review Letters*, 83(24):5162, 1999.
- [4] Sam McArdle, Suguru Endo, Alán Aspuru-Guzik, Simon C Benjamin, and Xiao Yuan. Quantum computational chemistry. *Reviews of Modern Physics*, 92(1):015003, 2020.
- [5] Ruizhe Zhang, Guoming Wang, and Peter Johnson. Computing ground state properties with early fault-tolerant quantum computers. *Quantum*, 6:761, 2022.
- [6] Rolando D Somma. Quantum eigenvalue estimation via time series analysis. *New Journal of Physics*, 21(12):123025, 2019.
- [7] Lin Lin and Yu Tong. Heisenberg-limited ground-state energy estimation for early fault-tolerant quantum computers. *PRX Quantum*, 3(1):010318, 2022.

[8] Guoming Wang, Daniel Stilck-Fran  a, Ruizhe Zhang, Shuchen Zhu, and Peter D Johnson. Quantum algorithm for ground state energy estimation using circuit depth with exponentially improved dependence on precision. *arXiv preprint arXiv:2209.06811*, 2022.

[9] Thomas E O’Brien, Brian Tarasinski, and Barbara M Terhal. Quantum phase estimation of multiple eigenvalues for small-scale (noisy) experiments. *New Journal of Physics*, 21(2):023022, 2019.

[10] Michael A Nielsen and Isaac Chuang. Quantum computation and quantum information, 2010.

[11] Zhiyan Ding and Lin Lin. Even shorter quantum circuit for phase estimation on early fault-tolerant quantum computers with applications to ground-state energy estimation. *PRX Quantum*, 4:020331, May 2023.

[12] Hongkang Ni, Haoya Li, and Lexing Ying. On low-depth algorithms for quantum phase estimation. *arXiv preprint arXiv:2302.02454*, 2023.

[13] Iulia M Georgescu, Sahel Ashhab, and Franco Nori. Quantum simulation. *Reviews of Modern Physics*, 86(1):153, 2014.

[14] Andrew M Childs and Yuan Su. Nearly optimal lattice simulation by product formulas. *Physical review letters*, 123(5):050503, 2019.

[15] Andrew M Childs, Yuan Su, Minh C Tran, Nathan Wiebe, and Shuchen Zhu. Theory of trotter error with commutator scaling. *Physical Review X*, 11(1):011020, 2021.

[16] Shelby Kimmel, Guang Hao Low, and Theodore J Yoder. Robust calibration of a universal single-qubit gate set via robust phase estimation. *Physical Review A*, 92(6):062315, 2015.

[17] Federico Belliardo and Vittorio Giovannetti. Achieving heisenberg scaling with maximally entangled states: An analytic upper bound for the attainable root-mean-square error. *Physical Review A*, 102(4), oct 2020.

[18] Zhiyan Ding and Lin Lin. Simultaneous estimation of multiple eigenvalues with short-depth quantum circuit on early fault-tolerant quantum computers. *arXiv preprint arXiv:2303.05714*, 2023.

[19] Haoya Li, Hongkang Ni, and Lexing Ying. On low-depth quantum algorithms for robust multiple-phase estimation. *arXiv preprint arXiv:2303.08099*, 2023.

[20] Emmanuel J Candès and Terence Tao. Near-optimal signal recovery from random projections: Universal encoding strategies? *IEEE transactions on information theory*, 52(12):5406–5425, 2006.

[21] Emmanuel J Candès, Justin K Romberg, and Terence Tao. Stable signal recovery from incomplete and inaccurate measurements. *Communications on Pure and Applied Mathematics: A Journal Issued by the Courant Institute of Mathematical Sciences*, 59(8):1207–1223, 2006.

[22] Emmanuel J Cand  s, Justin Romberg, and Terence Tao. Robust uncertainty principles: Exact signal reconstruction from highly incomplete frequency information. *IEEE Transactions on information theory*, 52(2):489–509, 2006.

[23] David Gross, Yi-Kai Liu, Steven T Flammia, Stephen Becker, and Jens Eisert. Quantum state tomography via compressed sensing. *Physical review letters*, 105(15):150401, 2010.

- [24] Anastasios Kyrillidis, Amir Kalev, Dohyung Park, Srinadh Bhojanapalli, Constantine Caramanis, and Sujay Sanghavi. Provable compressed sensing quantum state tomography via non-convex methods. *npj Quantum Information*, 4(1):36, 2018.
- [25] Gongguo Tang, Badri Narayan Bhaskar, Parikshit Shah, and Benjamin Recht. Compressed sensing off the grid. *IEEE transactions on information theory*, 59(11):7465–7490, 2013.
- [26] Clarice Poon, Nicolas Keriven, and Gabriel Peyré. The geometry of off-the-grid compressed sensing. *Foundations of Computational Mathematics*, 23(1):241–327, 2023.
- [27] Wenjing Liao and Albert Fannjiang. Music for single-snapshot spectral estimation: Stability and super-resolution. *Applied and Computational Harmonic Analysis*, 40(1):33–67, 2016.
- [28] Yohann De Castro and Fabrice Gamboa. Exact reconstruction using beurling minimal extrapolation. *Journal of Mathematical Analysis and applications*, 395(1):336–354, 2012.
- [29] Joel A Tropp et al. An introduction to matrix concentration inequalities. *Foundations and Trends® in Machine Learning*, 8(1-2):1–230, 2015.

7 Appendix

7.1 Proof of Lemma 1

Bernstein's inequality is stated as follows: Let X_1, X_2, \dots, X_N be independent zero-mean random variables. Suppose for all n , $|X_n| \leq \lambda$ almost surely, then for $t > 0$,

$$P \left(\left| \frac{1}{N} \sum_{n=1}^N X_n \right| \geq t \right) \leq 2 \exp \left(- \frac{N^2 t^2}{2 \sum_{n=1}^N E[X_n^2] + 2\lambda N t / 3} \right). \quad (74)$$

Using this inequality, we can prove the following lemma.

Lemma 3. *Given a fixed integer $k \in \mathbb{Z}_N^+$ and a random integer t in $[N]$, define a complex valued random variable*

$$Z = \exp(i2\pi kt/N), \quad (75)$$

then it satisfies the concentration bound

$$P \left(\left| \frac{1}{M} \sum_{m=1}^M Z_m \right| \geq \lambda \right) \leq 4 \exp \left(- \frac{3M\lambda^2}{8} \right). \quad (76)$$

Proof. We first rewrite this problem as a concentration problem for random matrices. Consider random variable

$$X = \begin{bmatrix} \cos(2\pi kt/N) & \sin(2\pi kt/N) \\ -\sin(2\pi kt/N) & \cos(2\pi kt/N) \end{bmatrix}. \quad (77)$$

We have

$$P \left(\left| \frac{1}{M} \sum_{m=1}^M Z_m \right| \geq \lambda \right) = P \left(\left\| \frac{1}{M} \sum_{m=1}^M X_m \right\| \geq \lambda \right), \quad (78)$$

where $\|\cdot\|$ is the largest singular value of the matrix. The new random variable satisfies

$$E[X] = 0, \quad \|X\| \leq 1, \quad \nu(X) = \sum_{m=1}^M E[X_m X_m^\dagger] = M. \quad (79)$$

Using the Theorem 1.6.1 in [29], we obtain for all $\lambda' \geq 0$

$$P \left(\left\| \sum_{m=1}^M X_m \right\| \geq \lambda' \right) \leq 4 \exp \left(\frac{-\lambda'^2/2}{M + \lambda'/3} \right), \quad (80)$$

which is equivalent to (set $\lambda' = \lambda/M$)

$$P \left(\left\| \frac{1}{M} \sum_{m=1}^M X_m \right\| \geq \lambda \right) \leq 4 \exp \left(\frac{-M\lambda^2/2}{1 + \lambda/3} \right) \leq 4 \exp \left(- \frac{3M\lambda^2}{8} \right). \quad (81)$$

The last inequality holds because when $\lambda > 1$, the probability is just 0 by the subadditivity of matrix norm, so the inequality is always true. Thus, we only consider the case where $\lambda \leq 1$. \square

Based on the previous lemma, we can prove Lemma 1 now.

Proof. By the definition of p , we can verify that $p_n = 1$. For all $k \neq n$, we have

$$p_k = \frac{1}{|\Omega|} \sum_{t=1}^{|\Omega|} X_t, \quad X_t = e^{i2\pi(k-n)r_t/N}, \quad (82)$$

where $\{r_t\}$ are random integers in $[N]$. For any $\varepsilon \in (0, 1)$, Lemma 3 ensures that

$$P(|p_k| > 1 - \varepsilon) \leq 4 \exp\left(-\frac{3|\Omega|(1 - \varepsilon)^2}{8}\right). \quad (83)$$

Thus, the probability of having $\forall k \neq n$, $|p_k| \leq 1 - \varepsilon$ is at least

$$\left[1 - 4 \exp\left(-\frac{3|\Omega|(1 - \varepsilon)^2}{8}\right)\right]^{N-1}. \quad (84)$$

Therefore, if we choose

$$|\Omega| \geq \frac{8}{3(1 - \varepsilon)^2} \ln\left(\frac{4(N - 1)}{\delta}\right), \quad (85)$$

p can serve as a dual certificate with probability at least $1 - \delta$. \square

7.2 Proof of Lemma 2

Proof. In this problem, we have

$$y_\Omega = y_\Omega^0 + z_\Omega, \quad y^0 = F^\dagger x, \quad x_k = \delta_{k,n}. \quad (86)$$

According to Lemma 1, if we set $|\Omega| \geq \lceil 32 \ln(4(N - 1)/\delta)/3 \rceil$, the dual certificate $p = F_\Omega y_\Omega^0 / |\Omega|$ satisfies

$$p_n = 1, \quad |p_k| \leq \frac{1}{2}, \quad \forall k \neq n \quad (87)$$

with probability at least $1 - \delta$. Calculate the inner product to obtain

$$\begin{aligned} \langle s^\#, p \rangle &= \frac{1}{|\Omega|} \langle s^\#, F_\Omega y_\Omega^0 \rangle \\ &= \frac{1}{|\Omega|} \langle F_\Omega^\dagger s^\#, y_\Omega^0 \rangle \\ &= \frac{1}{|\Omega|} \langle y_\Omega + \tilde{z}_\Omega, y_\Omega^0 \rangle \\ &= \frac{1}{|\Omega|} \langle y_\Omega^0 + z_\Omega + \tilde{z}_\Omega, y_\Omega^0 \rangle \\ &= 1 + \frac{1}{|\Omega|} \langle z_\Omega + \tilde{z}_\Omega, y_\Omega^0 \rangle. \end{aligned} \quad (88)$$

Here \tilde{z}_Ω comes from the fact that $F_\Omega^\dagger s^\# - y_\Omega$ can have a small deviation that satisfies $\|\tilde{z}_\Omega\|_2 \leq \sqrt{|\Omega|}\eta$. Furthermore,

$$\frac{1}{|\Omega|} |\langle z_\Omega, y_\Omega^0 \rangle| \leq \frac{1}{|\Omega|} \sum_{t \in \Omega} |z_t| \leq \frac{1}{\sqrt{|\Omega|}} \sqrt{\sum_{t \in \Omega} |z_t|^2} \leq \eta. \quad (89)$$

Thus,

$$1 - 2\eta \leq |\langle s^\#, p \rangle| \leq 1 + 2\eta. \quad (90)$$

On the other hand, x is a feasible solution, hence $\|s^\#\|_1 \leq \|x\|_1 = 1$, and

$$|\langle s^\#, p \rangle| \leq |s_n^\#| + \frac{1}{2} \sum_{k \neq n} |s_k^\#| \leq 1 - \frac{1}{2} \sum_{k \neq n} |s_k^\#|. \quad (91)$$

Combining them together, we obtain

$$\sum_{k \neq n} |s_k^\#| \leq 4\eta, \quad |s_n^\#| \geq 1 - 2\eta - \frac{1}{2} \sum_{k \neq n} |s_k^\#| \geq 1 - 4\eta. \quad (92)$$

□